Joint-Based Robotic Impedance Control Transformations: An Experimental Study

Carlos Saldarriaga[1][a], José J. Patiño[1][b], Carlos G. Helguero[1][c] and Imin Kao[2][d]

[1]*Facultad de Ingeniería en Mecánica y Ciencias de la Producción, Escuela Superior Politécnica del Litoral, ESPOL,
Campus Gustavo Galindo Km 30.5 Vía Perimetral, P.O. Box 09-01-5863, Guayaquil, Ecuador*
[2]*Department of Mechanical Engineering, Stony Brook University, Stony Brook, NY, U.S.A.*

Abstract: We present an experimental study in this paper to illustrate the effect of the Cartesian damping matrix on modulating the dynamic response of a robotic manipulator in impedance control. We first derive the transformation of the matrices of impedance control between the Cartesian and joint spaces using differential mathematics. Through experiments conducted on a redundant Franka Panda robot, it is demonstrated that the coupling term between damping and stiffness in impedance control derived from theoretical analysis, when transforming between the Cartesian and joint spaces, is important in stabilizing the dynamic response of the joints. We apply a methodology to modulate the dynamic response of a robot performing impedance control that allows us to study and select diagonal and off-diagonal elements of the Cartesian damping matrix according to the damping ratios and natural frequencies of the system in the modal space. In addition, we explain and show that an arbitrary selection of damping is counter-productive for robots to perform tasks under impedance control, and may lead to instability and out-of-range torques at the joints of the robotic manipulator.

1 INTRODUCTION

The main goal of impedance control at the task space level, and all its variations is to obtain a desired compliant behavior between the robot and its environment (Hogan, 1985; Khatib, 1987; Villani and De Schutter, 2008). In this type of controller, a mass-spring-damper relationship between task forces, **f**, and the errors of position and velocity of the end effector is used. There are basically two ways of implementing Cartesian impedance control (without inertia reshaping). One is by obtaining the interaction forces from the errors directly in the Cartesian space and then transform the forces into joint torques by equation (4). The other is by joint-based impedance control, where all the parameters are either given in the joint space or mapped from the Cartesian into the joint space, and the joint torques can be obtained directly in the joint space. A joint-based impedance control in combination with a closed-form solution of the multidimensional mechanical impedance system based on theory of mechanical vibrations (Saldarriaga et al., 2022a) allow us to analyze and synthesize the dynamics of the robot in a proper manner. Recent work on mechanisms using physical variable mechanical impedance elements (Vanderborght et al., 2013; Memar and Esfahani, 2018), have encouraged and given more relevance to the joint space analysis of robotic systems, making them more computationally efficient (Yu et al., 2019; Laffranchi et al., 2014). However, the main problem of this joint space analysis is the correct spatial transformation between Cartesian and joint spaces.

Although there is plenty of work on handling and design of non-diagonal stiffness matrices (Caccavale et al., 1999; Caccavale et al., 1998), and non-diagonal dominant inertia matrices for robotic impedance control (Pollayil et al., 2023), to the best of our knowledge, there is no work on off-diagonal elements for damping matrices.

Our methodology also allows us to select the elements of both stiffness and damping matrices, so that a desired dynamic behavior of the robot can be obtained. This tool can also be used to select off-diagonal values in the damping matrices to further im-

[a] https://orcid.org/0000-0001-9014-681X
[b] https://orcid.org/0000-0002-3740-352X
[c] https://orcid.org/0000-0002-6992-0572
[d] https://orcid.org/0000-0003-1658-9166

prove the damping ratios of the system in the modal space. The main advantages of our methodology include: (1) it can be used without losing generality; and (2) no assumptions of symmetry property of the involved matrices are made. This method is particularly useful for redundant manipulators.

A spatial transformation of both stiffness and damping was derived mathematically in (Saldarriaga et al., 2022b), which showed that damping in the Cartesian space is actually involved in the computation of stiffness in the joint space, along with the term from the conservative congruence transformation (Chen and Kao, 2000). An experimental study is proposed in this paper to show how this coupling term between stiffness and damping in the spatial transformation equation is important and can be beneficial and stabilizing in Cartesian impedance control tasks.

This paper is structured as follows: all the dynamics preliminaries and general control equations are presented in Section 2. After that, the mapping equations for stiffness and damping parameters are derived in Section 3. The dynamic response modulation methodology is explained in Section 4. The experimental results are presented in Section 5, with discussions and conclusion in Sections 6 and 7, respectively.

2 IMPEDANCE CONTROL

The equation of motion of an n-DoF (degree of freedom) manipulator is given by

$$\mathbf{M}(\mathbf{q})\ddot{\mathbf{q}}(t) + \mathbf{G}(\mathbf{q},\dot{\mathbf{q}})\dot{\mathbf{q}}(t) + \mathbf{v}(\mathbf{q}) = \boldsymbol{\tau}_m + \boldsymbol{\tau}_{ext} \quad (1)$$

here the vector $\mathbf{q}$ contains the n joint variables, $\mathbf{M}$ is the mass matrix, $\mathbf{G}$ is the matrix that contains the gyroscopic terms, $\mathbf{v}$ is the vector that compensates for gravity, and $\boldsymbol{\tau}_{ext}$ is the vector with the external torque values. To obtain a multi dimensional mass-damper-spring behavior we choose the motor torques $\boldsymbol{\tau}_{\mathbf{m}}$ as $[-\mathbf{K_q}\mathbf{q}(t) - \mathbf{C_q}\dot{\mathbf{q}}(t) + \mathbf{v}(\mathbf{q}) + \mathbf{G}(\mathbf{q},\dot{\mathbf{q}})\dot{\mathbf{q}}(t)]$, the system in equation (1) becomes

$$\mathbf{M}(\mathbf{q})\ddot{\mathbf{q}}(t) + \mathbf{C_q}\dot{\mathbf{q}}(t) + \mathbf{K_q}\mathbf{q}(t) = \boldsymbol{\tau}_{ext} \quad (2)$$

where $\mathbf{C_q}$ and $\mathbf{K_q}$ are the damping and stiffness matrices, respectively. The task space impedance control is performed according to the equation:

$$\mathbf{M}_C(\mathbf{q})\ddot{\mathbf{x}}(t) + \mathbf{C}_C\dot{\mathbf{x}}(t) + \mathbf{K}_C\mathbf{x}(t) = \mathbf{f} \quad (3)$$

where $\mathbf{K}_C$, $\mathbf{C}_C$, and $\mathbf{M}_C$ are the stiffness, damping, and mass matrices in the Cartesian space, correspondingly, and $\mathbf{f}$ stands for the force in the Cartesian space.

A very common implementation of impedance control is by imposing predefined stiffness and damping elements in the Cartesian space, then obtaining the required joint torques based on the errors from position and velocity with respect to the desired values, and applying these torques by the kineto-static relationship

$$\boldsymbol{\tau} = \mathbf{J}^T \mathbf{f} \quad (4)$$

added with the compensation of gravity and gyroscopic terms, similar as in (Ott, 2008; Kao and Saldarriaga, 2023) and illustrated in Figure 1, where:

$$\begin{aligned}
\boldsymbol{\tau}_c &= \mathbf{J}^T \left[\mathbf{K}_C(\mathbf{x} - \mathbf{x}_d) + \mathbf{C}_C(\dot{\mathbf{x}} - \dot{\mathbf{x}}_d) \right] \\
\boldsymbol{\tau} &= \boldsymbol{\tau}_c + \boldsymbol{\tau}_G
\end{aligned}$$

and $\boldsymbol{\tau}_G$ is the compensation of gravity and nonlinear terms.
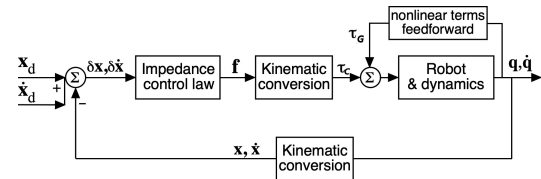

Figure 1: Block diagram of the Cartesian impedance controller.

The "Impedance control law" block in Figure 1 implements Equation (3) with the Cartesian force as the output. After the kinematic conversion block, the torque from impedance control law becomes $\boldsymbol{\tau}_c$. The nonlinear terms of the dynamic equation of motion are canceled by using a feedforward term $\boldsymbol{\tau}_G$, which is obtained from Equation (1), based on the current robot configuration.

On the other hand, one can also implement impedance control based directly on the joint space (joint-based impedance control). In this case, instead of obtaining and controlling $\mathbf{f}$ in Cartesian space and then transforming to torques via equation (4), the desired positions and its derivatives as well as the impedance parameters are given or computed directly in the joint space. An analysis and controller based on the joint space was needed in order to perform modal analysis of the redundant robot, where stiffness and damping become singular, and the only way to deal with this type of systems is by separating out the zero-potential energy (ZP) and non-zero-potential energy (NZP) modes of motion, using our methodology. This analysis allows us to obtain the torques directly in the joint space of the robot without losing generality. This analysis carried out in the joint space lets modulate the dynamic response of the robot through the impedance parameters directly at the joint level of the robot. The torque, $\boldsymbol{\tau}_c$, in this case is now

$$\boldsymbol{\tau}_c = \mathbf{K_q}(\mathbf{q} - \mathbf{q}_d) + \mathbf{C_q}(\dot{\mathbf{q}} - \dot{\mathbf{q}}_d) \quad (5)$$

3 MAPPING BETWEEN THE CARTESIAN AND JOINT SPACES

In this section, we present the derivation of the mapping of stiffness and damping matrices from the Cartesian space to the joint space for joint-based impedance control (Saldarriaga et al., 2022b). A generalized definition of stiffness and damping can be written as follows:

$$\mathbf{K} = \frac{\partial \mathbf{f}}{\partial \mathbf{x}} \tag{6}$$

$$\mathbf{C} = \frac{\partial \mathbf{f}}{\partial \dot{\mathbf{x}}} \tag{7}$$

where $\mathbf{f}$ denotes the force. From the generalization of a manipulator Jacobian matrix, we obtain

$$\delta \mathbf{x} = \mathbf{J} \, \delta \mathbf{q} \tag{8}$$

Taking derivative of (8) with respect to time through the chain rule, we obtain as follows

$$\frac{d}{dt}(\delta \mathbf{x}) = \mathbf{J}\frac{d}{dt}(\delta \mathbf{q}) + \dot{\mathbf{J}}\delta \mathbf{q} \tag{9}$$

From equations (6), (7) and (4) with a combined stiffness and damping control law, we can write the following equations

$$\delta \mathbf{f} = \mathbf{K}_C \, \delta \mathbf{x} + \mathbf{C}_C \frac{d}{dt}(\delta \mathbf{x}) \tag{10}$$

$$\delta \boldsymbol{\tau} = \mathbf{K_q} \, \delta \mathbf{q} + \mathbf{C_q}\frac{d}{dt}(\delta \mathbf{q}) \tag{11}$$

$$\delta \boldsymbol{\tau} = \delta \mathbf{J}^T \mathbf{f} + \mathbf{J}^T \delta \mathbf{f} \tag{12}$$

Substitute equations (10) and (11) into (12) to render

$$\delta \boldsymbol{\tau} = \delta \mathbf{J}^T \mathbf{f} + \mathbf{J}^T \left(\mathbf{K}_C \, \delta \mathbf{x} + \mathbf{C}_C \frac{d}{dt}(\delta \mathbf{x}) \right) \tag{13}$$

$$\mathbf{K_q} \, \delta \mathbf{q} + \mathbf{C_q}\frac{d}{dt}(\delta \mathbf{q}) = \delta \mathbf{J}^T \mathbf{f} + \mathbf{J}^T \mathbf{K}_C \delta \mathbf{x} + \mathbf{J}^T \mathbf{C}_C \frac{d}{dt}(\delta \mathbf{x}) \tag{14}$$

Substituting equations (8) and (9) into (14), we obtain

$$\begin{aligned} \mathbf{K_q} \, \delta \mathbf{q} + \mathbf{C_q}\frac{d}{dt}(\delta \mathbf{q}) = {} & \delta \mathbf{J}^T \mathbf{f} + \mathbf{J}^T \mathbf{K}_C \mathbf{J}\delta \mathbf{q} \\ & + \mathbf{J}^T \mathbf{C}_C \left(\mathbf{J}\frac{d}{dt}(\delta \mathbf{q}) + \dot{\mathbf{J}}\delta \mathbf{q} \right) \end{aligned} \tag{15}$$

$$\begin{aligned} \mathbf{K_q} \, \delta \mathbf{q} + \mathbf{C_q}\frac{d}{dt}(\delta \mathbf{q}) = {} & \delta \mathbf{J}^T \mathbf{f} + \mathbf{J}^T \mathbf{K}_C \mathbf{J}\delta \mathbf{q} \\ & + \mathbf{J}^T \mathbf{C}_C \mathbf{J}\frac{d}{dt}(\delta \mathbf{q}) + \mathbf{J}^T \mathbf{C}_C \dot{\mathbf{J}}\delta \mathbf{q} \end{aligned} \tag{16}$$

Since we know that $\mathbf{J}$ is a function of $\mathbf{q}$ but not $\dot{\mathbf{q}}$, we can rearrange $\delta \mathbf{J}^T \mathbf{f}$ and get

$$\mathbf{K}_G\delta \mathbf{q} = \left[\left(\frac{\partial \mathbf{J}^T}{\partial q_1}\mathbf{f} \right) \, \left(\frac{\partial \mathbf{J}^T}{\partial q_2}\mathbf{f} \right) \, ... \, \left(\frac{\partial \mathbf{J}^T}{\partial q_n}\mathbf{f} \right) \right] \delta \mathbf{q} \tag{17}$$

This $\mathbf{K}_G$ term represents the changes in geometry under the presence of external forces (Chen and Kao, 2000).

From equation (16), we can obtain the joint stiffness and damping matrices ($\mathbf{K_q}$, $\mathbf{C_q}$) by prescribed matrices in the Cartesian space ($\mathbf{K}_C$, $\mathbf{C}_C$)

$$\mathbf{K_q} = \mathbf{J}^T \mathbf{K}_C \mathbf{J} + \mathbf{K}_G + \mathbf{K}_B \tag{18}$$

$$\mathbf{C_q} = \mathbf{J}^T \mathbf{C}_C \mathbf{J} \tag{19}$$

where $\mathbf{K}_B = \mathbf{J}^T \mathbf{C}_C \dot{\mathbf{J}}$, it represents the changes in geometry due to the apparent velocity created, which generates an apparent stiffness matrix due to the damping matrix in impedance control. Mathematically, this term comes from the $\delta \mathbf{q}$ part of the equations, and contains the derivative of $\mathbf{J}$ with respect to time. For the rest of the paper, we refer to the first term on the right hand side of the equal sign in equation (18), $\mathbf{J}^T \mathbf{K}_C \mathbf{J}$, as the 'classical' or 'incomplete' transformation of stiffness.

Equations (18) and (19) describe the complete mapping of stiffness and damping of impedance control from the Cartesian space to the joint space, making equations (2) and (3) equivalent to each other. The matrices in the Cartesian space can be obtained with prescribed matrices in the joint space:

$$\mathbf{K}_C = \left(\mathbf{J}^T \right)^* (\mathbf{K_q} - \mathbf{K}_G - \mathbf{K}_B) \mathbf{J}^* \tag{20}$$

$$\mathbf{C}_C = \left(\mathbf{J}^T \right)^* \mathbf{C_q} \mathbf{J}^* \tag{21}$$

The superscript '*' in equations (20) and (21) represents the generalized inverse of the manipulator Jacobian $\mathbf{J}$, which is not square in case of redundancy ($n > m$) (Siciliano et al., 2010). Equations (18)-(21) form the "complete" mapping of impedance control between Cartesian and joint space. A convenient, derivative-free way of obtaining the extra terms in the stiffness transformation is by the screw-based Jacobian $\mathbf{J}$ (Muller, 2014).

4 DYNAMIC RESPONSE MODULATION THROUGH THE USE OF DAMPING

A very common way to select the damping parameters of impedance control is by a trial-and-error practice, with endless possibilities. In addition to being

cumbersome and a blind guess practice, this trial-and-error process can lead to undesired level of joint torques and highly unstable and dangerous systems. Furthermore, the trial-and-error process ignores the influence of the values of one damping parameter of the damping matrix on the others and the overall response. Instead, we propose to analyze the control criteria of the system in a modal space (Meirovitch, 2001) to regulate the dynamic response. As shown in (Saldarriaga et al., 2022a), once the system in equation (2) becomes positive definite (after the redundant ZP mode(s) is removed), the solution of dynamic response in the joint space is derived by using the linear system theory, with the following linear system equation

$$\dot{\mathbf{z}}(t) = \mathbf{A}\mathbf{z}(t) + \mathbf{B}\boldsymbol{\tau}_{ext}(t) \tag{22}$$

where

$$\mathbf{A} = \begin{bmatrix} \mathbf{0} & \mathbf{I} \\ -\mathbf{M}^{-1}\mathbf{K_q} & -\mathbf{M}^{-1}\mathbf{C_q} \end{bmatrix}, \mathbf{B} = \begin{bmatrix} \mathbf{0} \\ \mathbf{M}^{-1} \end{bmatrix} \tag{23}$$

The solution of equation (22) assumes the following form

$$\begin{aligned} \mathbf{z}(t) &= \begin{bmatrix} \mathbf{q}(t) \\ \dot{\mathbf{q}}(t) \end{bmatrix} = \mathbf{X}e^{\boldsymbol{\Lambda}t}\mathbf{Y}^{T}\mathbf{z}(0) \\ &+ \int_{0}^{t} \mathbf{X}e^{\boldsymbol{\Lambda}\tau}\mathbf{Y}^{T}\mathbf{B}\tau_{ext}(t-\tau)d\tau \end{aligned} \tag{24}$$

where $\mathbf{X}$ and $\mathbf{Y}$ are the right and left eigenvectors of the matrix $\mathbf{A}$, and $\boldsymbol{\Lambda}$ is a diagonal matrix with all the eigenvalues of $\mathbf{A}$.

The details of the methodology for one redundant DoF can be found in (Saldarriaga et al., 2022a). We can obtain every damping ratio ζ_i, corresponding to every eigenvalue (mode) of the $\mathbf{A}$ matrix, and we can improve them in a theoretically sound systematic manner by selecting proper elements of stiffness and damping. By performing a parameter study of each element of the damping matrix, we can analyze and determine the elements (diagonal or off-diagonal) that have most effect on the dynamic response and specifically on which modes. Thus, we can choose stiffness and damping parameters to modulate the dynamic response in a deterministic manner, without any assumptions or trial and error.

5 EXPERIMENTS

For a given starting configuration $\mathbf{q}_0 = [0; -\pi/4; 0; -3\pi/4; 0; \pi/2; \pi/4] rad$ of the Panda robot, a circular path is commanded at the end-effector level ($m = 6$) for 13 seconds at a constant speed for several cycles with a specified set of Cartesian stiffness and damping parameters, $\mathbf{K}_C$ and $\mathbf{C}_C$,

respectively, using joint-based impedance control. This circle is in the *XY* Cartesian space, as shown in Fig 2. At each iteration the inverse kinematics function of the Panda controller obtains a desired robot joint configuration based on the intended path, as the robot moves along this plane. The Jacobian matrix $\mathbf{J}$ also changes, which has an impact on the joint stiffness and damping matrices $\mathbf{K_q}$ and $\mathbf{C_q}$, respectively, with the prescribed $\mathbf{K}_C$ and $\mathbf{C}_C$ in the Cartesian space, as shown in equations (18) and (19).
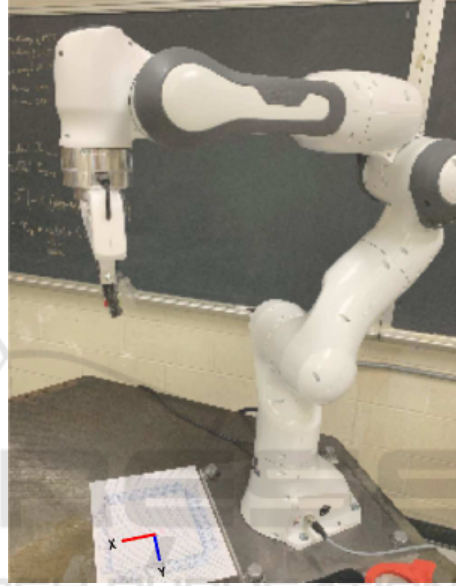

Figure 2: 7 DoF Panda robot used in the experiments.

For these experiments, given that no external forces are being applied (other than the torques generated by the robot joints itself), we are going to neglect the computation of the $\mathbf{K}_G$ term in equation (18), and will focus on the importance of the $\mathbf{K}_B$ term on both the stiffness transformation and the intended robotic task in the Cartesian space in two different situations: (1) arbitrary or trial-and-error damping, and (2) diagonal proper damping. From a higher perspective, impedance control is a trade-off or compromise between force control and position control, we chose to test it by tracing a prescribed trajectory, to some extent similar to position control without external forces maintaining a mechanical compliance level.

The chosen Cartesian stiffness matrix for the robotic task was $\mathbf{K}_C = \text{diag}(3000, 5000, 12000, 100, 150, 100)$ in SI units for both position and orientation.

5.1 Arbitrary Damping Matrix

Another common practice to select a set of damping parameters in a robotic system performing impedance control is to assume a diagonal mass matrix $\mathbf{M}$ and impose $\mathbf{C}_{C1} = 2\sqrt{\mathbf{K}_C}$ (similar to the impedance example code provided by the manufacturer). As we can see in the Appendix, the mass matrix is far from being diagonal. For this case, the Panda robot became highly unstable once we used this arbitrary damping matrix $\mathbf{C}_{C1}$. Torques and velocities in the joints can become out of range with bifurcation, the actuators cannot keep up with the controller. The robot can crash with no data being collected.
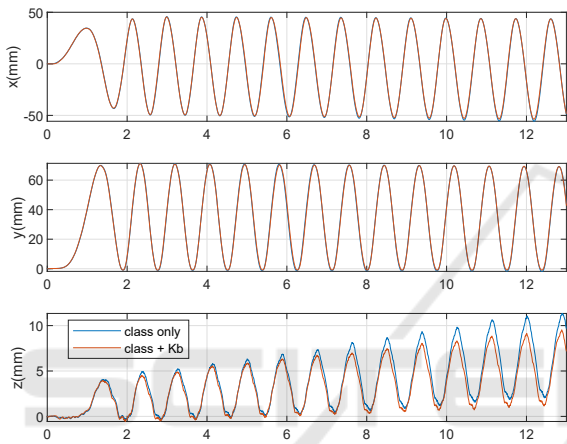

Figure 3: Results in the Cartesian space using an arbitrary choice of damping matrix with $\mathbf{C}_{C2} = \sqrt{\mathbf{K}_C}$. Comparison between the classical (in blue) and equation (18) with $\mathbf{K}_B$ term (in red).
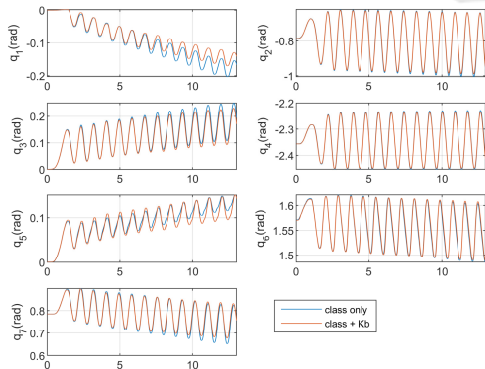

Figure 4: Results of joint angles using an arbitrary choice of damping matrix with $\mathbf{C}_{C2} = \sqrt{\mathbf{K}_C}$. Comparison between the classical (in blue) and equation (18) with $\mathbf{K}_B$ term (in red).

Another arbitrary damping matrix was chosen with half of the values of the previous choice with $\mathbf{C}_{C2} = \sqrt{\mathbf{K}_C}$. The experimental results of the Cartesian positions are plotted in Figure 3 for multiple cy-

cles. Since the displacement is intended in the XY plane, the displacement in the Z direction should be very small, but this is clearly not the case, and gets worse over time. The joint angles are plotted in Figure 4. The joint angles are drifting with multiple cycles of movement, and significantly affecting the Cartesian positions. The addition of $\mathbf{K}_B$ using equation (18) helps in reducing or stabilizing the response but it is not ideal due to the selection of this arbitrary damping matrix.

5.2 Appropriately Chosen Damping Matrix

As explained in Section 4, the diagonal damping parameters are chosen keeping in mind the effect that each element has on each of the damping ratios and natural frequencies in the modal space once the redundancy of the robot or ZP mode (Saldarriaga et al., 2022a) is taken care of, without imposing high values of damping matrix that lead to over-damped or very slow motions. After a parameter study of the elements of $\mathbf{C_C}$, the chosen diagonal damping matrix was $\mathbf{C}_C = \mathrm{diag}(20, 30, 40, 12, 22, 0.75)$ in SI units for both position and orientation. This set of stiffness and damping matrices generates the following damping ratios and natural frequencies in the modal space:

$$\boldsymbol{\zeta} = \begin{bmatrix} 0.089 \\ 0.20 \\ 0.26 \\ 1+ \\ 1+ \\ 0.68 \end{bmatrix} \; ; \; \boldsymbol{\omega}_n = \begin{bmatrix} 49.1 \\ 15.0 \\ 31.8 \\ - \\ - \\ 179 \end{bmatrix} rad/s$$

the overdamped pairs correspond to the overdamped roots, where $\zeta \geq 1$.

From Figures 5 and 6 we can see how the response of the robot is improved; especially, there is significantly less drift at the joints when the $\mathbf{K}_B$ term is included. In addition, more acceptable movement in the Z direction is found with $\mathbf{K}_B$ term. However, the damping ratio of mode 1-2 is still low and might yield better results when increased.

6 DISCUSSIONS

Equations (18) and (19), derived mathematically to provide a transformation of stiffness and damping matrices of impedance control between the Cartesian and joint spaces, enable us to correctly compute the stiffness and damping matrices in the joint space. As shown in the experiments in Section 5, the classical incomplete transformation leads to torque errors that
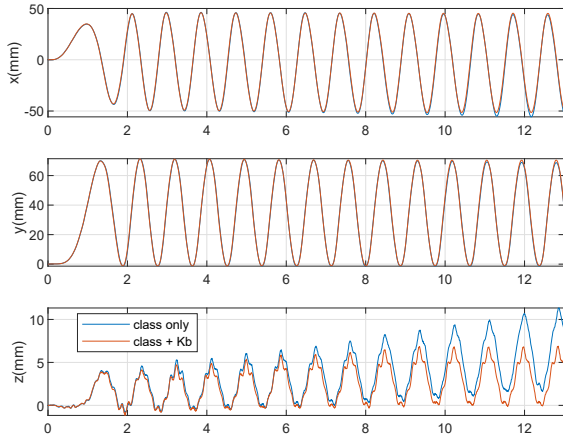
Figure 5: Results in the Cartesian space using an appropriately chosen diagonal damping matrix $\mathbf{C}_C$. Comparison between the classical (in blue) and equation (18) with $\mathbf{K}_B$ term (in red).
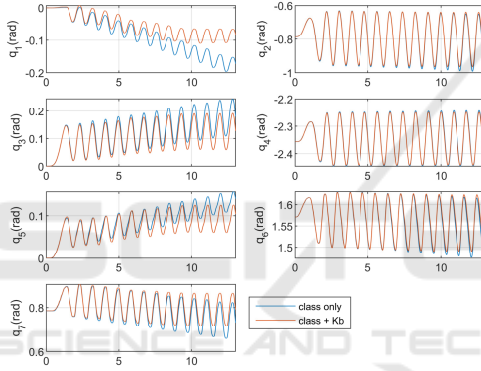

Figure 6: Results of joint angles using an appropriately chosen diagonal damping matrix. Comparison between the classical (in blue) and equation (18) with $\mathbf{K}_B$ term (in red).

have a negative impact on a robotic impedance task. On the other hand, including the coupling term $\mathbf{K}_B$ in the transformation equation yields a better dynamic response, which quickly settles down after a transition period. In comparison, the classical or incomplete transformation leads to a joint response that drifts indefinitely.

Based on the fundamental differential mathematics and the use of the chain rule, we derived the transformation equation (18) for stiffness including a term that involves the damping matrix in the Cartesian space and the derivative of the Jacobian matrix. It showed up in the stiffness because of the apparent velocity due to the change in Jacobian, which creates an equivalent term of apparent damping in stiffness. This apparent velocity due to the change in Jacobian is not an actual physical velocity; hence, it does not generate a dissipative effect, and the conservative property of stiffness is maintained.

Equations (22) to (24) are used to obtain the dynamic response of the system under impedance control. The methodology employed to select the individual elements of the damping matrix enables us to modulate the dynamic response, provided by equation (24), by changing the damping ratios in the modal space of the system matrix $\mathbf{A}$ in equation (23) (Saldarriaga et al., 2022a). It is very important to maintain stability by ensuring that none of the eigenvalues of the modal space are in the right-half part of the complex plane.

Employing the parameter study, we found that also the off-diagonal elements can be used to increase even more the intended damping ratio. For example, looking at Subsection 5.2, the damping ratio corresponding to mode 1-2 increases when increasing the element $(3,5)$ of the damping matrix $\mathbf{C}_C$, as shown in Figure 7.

If we choose the element $(3,5)$ of the Cartesian damping matrix $\mathbf{C}_C$ to be 55, we obtain the following damping ratios and natural frequencies in the modal space:

$$\boldsymbol{\zeta} = \begin{bmatrix} 0.1037 \\ 0.20 \\ 0.26 \\ 1+ \\ 1+ \\ 0.68 \end{bmatrix} ; \quad \boldsymbol{\omega}_n = \begin{bmatrix} 51.6 \\ 15.1 \\ 31.8 \\ - \\ - \\ 179 \end{bmatrix} rad/s$$

In case of working with non-symmetric matrices, either $\mathbf{C}_C$ or $\mathbf{K}_C$, or both, we need to make sure that the positive-definiteness is always maintained. For any $\mathbf{K}_1$ matrix, the condition: $\mathbf{y}_1^T \mathbf{K}_1 \mathbf{y}_1 > 0$ must be held for all $\mathbf{y}_1 \in \Re^{n \times 1}$ (Strang, 2009) to ensure a positive definite $\mathbf{K}_1$ matrix. Note that when imposing certain off-diagonal values in $\mathbf{C}_C$, this condition may not be satisfied and a more careful selection of parameters needs to be done, which can also be accounted for when generating the sets of parameter study using our methodology.

Positive-definiteness is a property that has not been extensively studied on Non-symmetric matrices, similar to the one in the case of element $(3,5)$ of the damping matrix. It is known that obtaining positive eigenvalues is a sure consequence of dealing with positive definite real matrices. That is precisely a characteristic of the non-diagonal matrix chosen in the experimental work, the eigenvalues of the reduced damping matrix are all positive ($\boldsymbol{\lambda}$=[1.316 7.289 8.514 14.65 23.18 8515248]), which brings the stability and consistency needed for the system. This can only be accounted for by using our methodology.

We also saw how the Cartesian stiffness values, especially in X and Y (3000 and 5000, which were chosen for illustration and generalization purposes only), affect the actual displacement of the end-

effector, regardless of the intended circular path for the impedance task.

As counterintuitive as it may sound, using higher damping parameters does not necessarily mean that the resulting damping ratios become higher as well. This is clearly one of the main advantages of using the proposed methodology to determine exactly which element needs to be increased to modulate the damping behavior of the system.

One of the assumptions made in the analysis and implementation is that the changes in the Jacobian matrix **J** are relatively small, which to some extent and for the experiments performed here it might work relatively fine, but once the displacements become larger, as expected from theory, the damping matrix can no longer be kept constant for a given task. The feature of an analytically obtained, time and configuration dependent damping matrix tackling this limitation is part of our current work.

The apparent stiffness term, $\mathbf{K}_B$ in the stiffness transformation equation (18), involving the damping matrix has a stabilizing effect in the response of the robot performing impedance control, as it contains information on how the Jacobian matrix with configuration changes over time.
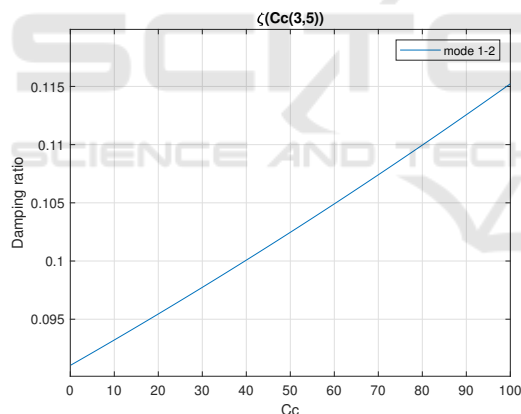

Figure 7: Parameter study of the (3,5) element of $\mathbf{C}_C$. Damping ratio in the modal space as a function of the element (3,5) of the Cartesian damping matrix $\mathbf{C}_C$.

In the present study we have found an unexpected drift in the experimental results for the Z direction, which given the relatively large stiffness value in that Cartesian direction, should not be there. We saw that the drift is larger and more evident in the cases that do not consider the coupling term, further investigation and considerations must be given to this result, and it is also part of our future work.

7 CONCLUSION

In this paper, we derived the equations to transform stiffness and damping matrices in impedance control between the Cartesian and joint spaces and show experimentally the effectiveness of the proposed theory, in comparison with the incomplete classic transformation. We also demonstrated that the stiffness matrix term, $\mathbf{K}_B$, derived mathematically due to the apparent velocity from the change in Jacobian matrix in manipulation under impedance control, is very important and has a stabilizing effect in manipulation and motion for the robotic manipulator. In addition, the solution methodology based on the linear system theory allows us to modulate the dynamic response of the system by increasing the damping ratios in the modal space, through the change of symmetric and non-symmetric elements of the damping matrix in impedance control.

REFERENCES

Caccavale, F., Siciliano, B., and Luigi, V. (1998). Quaternion-based impedance with nondiagonal stiffness for robot manipulators. volume 1, pages 468 – 472 vol.1.

Caccavale, F., Siciliano, B., and Villani, L. (1999). Robot impedance control with nondiagonal stiffness. *IEEE Transactions on Automatic Control*, 44(10):1943–1946.

Chen, S.-F. and Kao, I. (2000). Conservative congruence transformation for joint and cartesian stiffness matrices of robotic hands and fingers. *The International Journal of Robotics Research*, 19(9):835–847.

Hogan, N. (1985). Impedance control: An approach to manipulation: part i - theory, part ii - implementation, part iii - applications. *Journ. of Dyn. Systems, Measurement and Control*, 107(1):1–24.

Kao, I. and Saldarriaga, C. (2023). Manipulation(to be published). In Siciliano, B., editor, *Springer Handbook of Robotics, MOOCS*. Springer, Berlin, Heidelberg.

Khatib, O. (1987). A unified approach for motion and force control of robot manipulators: The operational space formulation. *IEEE Journal on Robotics and Automation*, 3(1):43–53.

Laffranchi, M., Chen, L., Kashiri, N., Lee, J., Tsagarakis, N., and Caldwell, D. (2014). Development and control of a series elastic actuator equipped with a semi active friction damper for human friendly robots. *Robotics and Autonomous Systems*, 62(12):1827 – 1836.

Meirovitch, L. (2001). *Fundamentals of Vibrations*. McGraw-Hill.

Memar, A. H. and Esfahani, E. T. (2018). A variable stiffness gripper with antagonistic magnetic springs for enhancing manipulation. In *Robotics: Science and Systems*.

Muller, A. (2014). Higher derivatives of the kinematic mapping and some applications. *Mechanism and Machine Theory*, 76:70 – 85.

Ott, C. (2008). *Cartesian Impedance Control of Redundant and Flexible-Joint Robots*. Springer Publishing Company, Incorporated, 1 edition.

Pollayil, M. J., Angelini, F., Xin, G., Mistry, M., Vijayakumar, S., Bicchi, A., and Garabini, M. (2023). Choosing stiffness and damping for optimal impedance planning. *IEEE Transactions on Robotics*, 39(2):1281–1300.

Saldarriaga, C., Chakraborty, N., and Kao, I. (2022a). Damping selection for cartesian impedance control with dynamic response modulation. *IEEE Transactions on Robotics*, 38(3):1915–1924.

Saldarriaga, C., Chakraborty, N., and Kao, I. (2022b). Joint space stiffness and damping for cartesian and null space impedance control of redundant robotic manipulators. In Asfour, T., Yoshida, E., Park, J., Christensen, H., and Khatib, O., editors, *Robotics Research*, pages 410–426, Cham. Springer International Publishing.

Siciliano, B., Sciavicco, L., Villani, L., and Oriolo, G. (2010). *Robotics: Modelling, Planning and Control*. Advanced Textbooks in Control and Signal Processing. Springer London.

Strang, G. (2009). *Introduction to Linear Algebra*. Wellesley-Cambridge Press, fourth edition.

Vanderborght, B., Albu-Schaeffer, A., Bicchi, A., Burdet, E., Caldwell, D., Carloni, R., Catalano, M., Eiberger, O., Friedl, W., Ganesh, G., Garabini, M., Grebenstein, M., Grioli, G., Haddadin, S., Hoppner, H., Jafari, A., Laffranchi, M., Lefeber, D., Petit, F., Stramigioli, S., Tsagarakis, N., Damme, M. V., Ham, R. V., Visser, L., and Wolf, S. (2013). Variable impedance actuators: A review. *Robotics and Autonomous Systems*, 61(12):1601 – 1614.

Villani, L. and De Schutter, J. (2008). Force control. In Siciliano, B. and Khatib, O., editors, *Springer Handbook of Robotics*, pages 161–185. Springer, Berlin, Heidelberg.

Yu, J., Zhao, Y., Chen, G., Gu, Y., Wang, C., and Huang, S. (2019). Realizing controllable physical interaction based on an electromagnetic variable stiffness joint. *Journal of Mechanisms and Robotics*, 11(5):054501.

$$\mathbf{M(q)} = \begin{bmatrix} 0.5031 & -0.006 & 0.4756 & -0.0024 & 0.0527 & -0.0005 & -0.0028 \\ -0.006 & 1.5460 & -0.0225 & -0.6848 & -0.0078 & -0.0335 & -0.0009 \\ 0.4756 & -0.0225 & 0.9674 & -0.0146 & 0.0615 & 0.0007 & -0.0034 \\ -0.0024 & -0.6848 & -0.0146 & 0.9442 & 0.0208 & 0.1187 & 0.0012 \\ 0.0527 & -0.0078 & 0.0615 & 0.0208 & 0.0229 & -0.0015 & 0.0021 \\ -0.0005 & -0.0335 & 0.0007 & 0.1187 & -0.0015 & 0.0444 & 0.0013 \\ -0.0028 & -0.0009 & -0.0034 & 0.0012 & 0.0021 & 0.0013 & 0.003 \end{bmatrix}$$

APPENDIX

The Jacobian and mass inertia matrices of the Panda robot at the starting configuration used for the analyses were:

$$\mathbf{J(q)} = \begin{bmatrix} -0.0002 & 0.1525 & -0.0001 & 0.1293 & 0 & 0.2106 & 0 \\ 0.3066 & 0 & 0.3247 & 0.0001 & 0.2104 & -0.0001 & 0 \\ 0 & -0.3066 & -0.0002 & 0.4717 & 0.0001 & 0.0875 & 0 \\ 0 & 0.0001 & -0.7070 & 0 & 1 & 0 & -0.0025 \\ 0 & 1 & 0.0001 & -1 & 0 & -1 & 0.0007 \\ 1 & 0 & 0.7072 & 0.0001 & -0.003 & -0.0007 & -1 \end{bmatrix}$$